JOURNAL OF BACTERIOLOGY, June 2007, p. 4359–4366 Vol. 189, No. 12
0021-9193/07/$08.00+0 doi:10.1128/JB.00132-07

SOS Induction in a Subpopulation of Structural Maintenance of Chromosome (Smc) Mutant Cells in *Bacillus subtilis*▽†

Robert A. Britton,‡ Elke Küster-Schöck,§ Thomas A. Auchtung,¶ and Alan D. Grossman*

Department of Biology, Building 68-530, Massachusetts Institute of Technology, Cambridge, Massachusetts 02139

Received 26 January 2007/Accepted 2 April 2007

The structural maintenance of chromosome (Smc) protein is highly conserved and involved in chromosome compaction, cohesion, and other DNA-related processes. In *Bacillus subtilis*, *smc* null mutations cause defects in DNA supercoiling, chromosome compaction, and chromosome partitioning. We investigated the effects of *smc* mutations on global gene expression in *B. subtilis* using DNA microarrays. We found that an *smc* null mutation caused partial induction of the SOS response, including induction of the defective prophage PBSX. Analysis of SOS and phage gene expression in single cells indicated that approximately 1% of *smc* mutants have fully induced SOS and PBSX gene expression while the other 99% of cells appear to have little or no expression. We found that induction of PBSX was not responsible for the chromosome partitioning or compaction defects of *smc* mutants. Similar inductions of the SOS response and PBSX were observed in cells depleted of topoisomerase I, an enzyme that relaxes negatively supercoiled DNA.

Chromosome compaction and organization are necessary for DNA replication and chromosome partitioning to function properly. Structural maintenance of chromosome (Smc) proteins are highly conserved and function in a variety of processes that involve DNA, including recombination, repair, and transcription (16–18). First identified in eukaryotes, Smc proteins are members of protein complexes involved in chromosome condensation (condesin) and sister chromatid cohesion (cohesin) (14).

Smc is found in most gram-positive and several gram-negative bacteria (34). Smc plays an important role in chromosome structure and organization in *Bacillus subtilis*. *B. subtilis smc* null mutants have pleiotropic phenotypes, including abnormal chromosome partitioning, poorly compacted nucleoids, mispositioning of origin and terminus regions, slow growth, and the inability to form colonies above 25°C when grown on rich media (5, 23, 31). *smc* mutations are synthetic when combined with other mutations that also affect chromosome partitioning, including *spoIIIE* (4), *spo0J* (4), *soj* (21), and *prfA* (32).

B. subtilis Smc forms a complex with two proteins, ScpA and ScpB (9, 26, 35, 38). *scpA* and *scpB* null mutants have phenotypes that are nearly identical to that of *smc* null mutants (35). Identification of proteins that directly interact with ScpA led to the hypothesis that the Smc-ScpA-ScpB complex also participates in DNA repair and gene expression controlled by the two-component signal transduction system, DegS and DegU (9).

We were interested in investigating the role of *smc* in global gene expression, as well as in learning more about other phenotypic changes that occur in *smc* mutants. We used DNA microarrays to analyze the effects of *B. subtilis smc* null mutations on gene expression during growth. At the same time, we identified genes affected by *ftsY* (also known as *srb*, the gene immediately downstream from *smc*), which encodes an essential component of the signal recognition particle involved in protein secretion.

Our results indicate that during growth in *smc* null mutants there is partial induction of the SOS response. The SOS response is a global regulatory response to DNA damage and disruptions in DNA replication. In *B. subtilis*, this response causes changes in the expression of over 600 genes (12, 13), including induction of some lysogenic phage (including the defective prophage PBSX) and the integrative and conjugative element ICE*Bs1* (see references 2 and 12 and references therein). The bulk of the transcriptional response is caused by activation of RecA, which facilitates inactivation of various transcriptional repressors, including LexA and some phage repressors. LexA directly represses the expression of approximately 60 genes in 26 operons in *B. subtilis* (1, 12). Analysis of gene expression in single cells indicated that the SOS response is activated in a subpopulation of *smc* mutant cells.

MATERIALS AND METHODS

Strains, alleles, and plasmids. *B. subtilis* strains are listed in Table 1. All are derivatives of JH642 (*trp phe*) unless otherwise indicated. Δ*smc*::*kan* (in strain RB35) is a deletion-insertion in *smc* (Fig. 1) (5). *smc*::pRB7 (in strain RB27) is a single-crossover disruption of *smc* with an internal fragment of *smc* cloned into pGEM*cat* (pRB7) (5). The *scpA* null mutation was previously described (24, 35).

ftsY::pDL53 (in strain RB25) is a single-crossover integration that results in the insertion of pGEM*cat* (pDL53) between *smc* and *ftsY* (5). The resulting strain is *smc*$^+$ but has separated *ftsY* from its native promoter. The integration of pRB7 (in *smc*) and pRB53 (in *ftsY*) results in the same genome arrangement downstream of the plasmid in RB27 and RB25, causing *ftsY* to be removed from its normal transcriptional regulation.

P_{spac}-*topA* puts the only copy of *topA*, encoding topoisomerase I (Topo I), under control of the IPTG (isopropyl-β-D-thiogalactopyranoside)-inducible promoter P_{spac} and was previously described (23).

* Corresponding author. Mailing address: Department of Biology, Building 68-530, Massachusetts Institute of Technology, Cambridge, MA 02139. Phone: (617) 253-1515. Fax: (617) 253-2643. E-mail: adg@mit.edu.

† Supplemental material for this article may be found at http://jb.asm.org/.

‡ Present address: Department of Microbiology and Molecular Genetics, Michigan State University, East Lansing, MI 48824.

§ Present address: Department of Biology, McGill University, Montreal, QC, Canada.

¶ Present address: Department of Organismal and Evolutionary Biology, Harvard University, Cambridge, MA 02138.

▽ Published ahead of print on 6 April 2007.

TABLE 1. *B. subtilis* strains

Strain	Relevant genotype (reference[s])
AG174	*trp phe*; wild-type strain (also known as JH642)
JCL245	P_{spac}-*topA* (23)
RB25	*ftsY*::pDL53; pDL53 inserted between *smc* and *ftsY* and partly polar on *ftsY* (5)
RB27	Δ*smc*::pRB7; disruption of *smc* and partly polar on *ftsY* (5)
RB35	Δ*smc*::*kan*; deletion-insertion in *smc* and partly polar on *ftsY* (5)
RB98	*tagC-gfp cat*
RB151	Δ*smc*::*kan xin-1* SPβ^0 ICE*Bs1*^{0} (YB886 background)
RB164	Δ*smc*::*kan xkdF-yfp* (*spc*)
RB169	Δ*smc*::*kan tagC-gfp* (*cat*)
RB171	Δ*scpA*::*mls* (AG174 background) (24, 35)
RB173	*xin-1 xkdF-yfp* (*spc*) SPβ^0 (AG174 background)
RB175	Δ*scpA*::*mls xin-1 xkdF-yfp* (*spc*) SPβ^0 (AG174 background)
RB177	Δ*smc*::*kan* (*smc ftsY*) *xin-1 xkdF-yfp* (*spc*) SPβ^0 (AG174 background)
RB178	*xkdF-yfp* (*spc*)
RB179	Δ*scpA*::*mls xkdF-yfp* (*spc*)
RB243	P_{spac}-*topA xkdF-yfp* (*spc*)
RB244	*xkdF-yfp* (*spc*) *ftsY*::pDL53
YB886	*xin-1* SPβ^0 ICE*Bs1*^{0} *amyE sigB metB trpC* (2, 7, 29, 40)

tagC-gfp was made by amplifying a 3′ fragment of *tagC* and cloning it into the vector pPL52, which contains a *spo0J-gfp* fusion and *cat*. The *spo0J* fragment was removed and replaced with the 3′ end of the *tagC* gene. The resulting plasmid was integrated into the chromosome at *tagC* by a single crossover selecting for chloramphenicol resistance, generating strain RB98.

xkdF-yfp was created by cloning a 3′ fragment of *xkdF* in frame with *yfp*, resulting in plasmid pJL77. The resulting plasmid was introduced by transformation into a wild-type laboratory strain, AG174 (JH642), by selecting for spectinomycin resistance, generating strain RB178.

RB151 (Δ*smc*::*kan xin-1* SPβ^0) contains the Δ*smc*::*kan* mutation in strain YB886. YB886 is cured of the lysogenic phage SPβ and contains *xin-1*, a mutation in the defective phage PBSX that prevents induction of PBSX (7, 29, 40) and is cured of the integrative and conjugative element ICE*Bs1* (2).

RB173 (SPβ^0 *xin-1 xkdF-yfp spc*) was constructed by taking AG174, which had been cured of SPβ, and introducing the *xin-1* mutation by transformation. First, the *xkdF-yfp* plasmid (pJL77) was integrated into *xkdF* in strain YB886, selecting for spectinomycin resistance. Chromosomal DNA from this strain was used to transform the SPβ^0 AG174 strain to spectinomycin resistance (*xkdF-yfp spc*). A high concentration of DNA was used to favor congression (cotransfer of unlinked markers) because it is not known which gene contains the *xin-1* mutation. Most likely, *xin-1* is in *xre* (which encodes the PBSX repressor), which is located ~8 kb away from *xkdF* and should be weakly linked by transformation. However, if *xin-1* is significantly farther from *xkdF*, then it is may not be linked by transformation and the DNA concentration used in the transformation should allow for congression. Strains that induce PBSX cause the cell to lyse after treatment with the DNA-damaging agent mitomycin C (MMC). Spectinomycin-resistant transformants were tested for cell lysis after treatment with 1 μg/ml mitomycin C. Three of 50 transformants did not lyse, indicating that they had acquired the *xin-1* mutation and were unable to induce PBSX. Their inability to express PBSX was confirmed by the loss of *xkdF-yfp* expression and the loss of PBSX gene expression when treated with MMC. The apparent linkage between *xin-1* and *xkdF-yfp* is most consistent with cotransformation of weakly linked markers. However, this cotransformation frequency could also be indicative of a relatively high level of congression. RB177 (Δ*smc*::*kan xin-1* SPβ^0 *xkdF-yfp*) was made by introducing Δ*smc*::*kan* into RB173 by transformation.

Media and growth conditions. Cells were grown in defined minimal medium containing S7 minimal salts (37) (with 50 mM MOPS instead of 100 mM) supplemented with 1% glucose, 0.1% glutamate, and required amino acids. For experiments involving *smc* mutants, cells were grown at 30°C unless otherwise noted. Drugs were added as appropriate at the following concentrations: kanamycin, 5 μg/ml; spectinomycin, 100 μg/ml; chloramphenicol, 5 μg/ml; mitomycin C, 1 μg/ml.

DNA microarray analysis. The DNA microarrays used in this study were previously described (3). Briefly, PCR products for 4,074 of the 4,106 genes of *B. subtilis* were amplified with primers designed by Sigma-Genosys. The DNA was printed on CMT-GAPS II slides (Corning). Cells were grown to mid-exponential phase (optical density at 600 nm [OD_{600}], ~0.7), mixed with an equal volume of −20°C methanol for 2 min, pelleted, and frozen at −80°C until RNA was prepared with an RNeasy mini kit (QIAGEN). Ten micrograms of RNA was reverse transcribed into labeled cDNA by either direct incorporation of Cy3 and Cy5 dUTP or indirect labeling using aminoallyl dUTP followed by chemical coupling of Cy3 or Cy5. Data were captured with a GenePix 4000B scanner (Axon), and images were processed with GenePix Pro 3.0 software. At least three biological replicates were performed for each experiment. Data were normalized to the total signal of each channel. Iterative outlier analysis was performed to identify genes that were significantly changed in relationship to the population (3, 25). Genes that were 2.5 standard deviations from the population were considered significantly altered in expression.

Two types of experiments were performed to distinguish the effects on gene expression due to *smc*. mRNA was compared directly between *smc* null mutant (Δ*smc*::*kan*; RB35) and wild-type cells. After observing a polar effect on *ftsY*, we did experiments to evaluate effects caused by *ftsY*. In these experiments, gene expressions in Δ*smc*::*kan* (RB35), *smc*::pRB7 (RB27), and *smc*$^+$ *ftsY*::pDL53 (RB25) strains were compared to a common reference wild-type (AG174) RNA. This allowed for straightforward comparisons of gene expression between the three strains. Five different data sets were generated for analysis: (i) Δ*smc*::*kan* (RB35) versus the wild type (AG174) (direct comparison on the array), (ii) Δ*smc*::*kan* (RB35) versus reference RNA, (iii) *smc*::pRB7 (RB27) versus reference RNA, (iv) AG174 versus reference RNA, and (v) *smc*$^+$ *ftsY*::pDL53 (RB25) versus reference RNA.

To identify genes whose expression was altered specifically due to the loss of *smc* and not due to decreased expression of *ftsY*, we required that a gene be identified in the iterative outlier analysis in two of the three experiments [RB35 (Δ*smc*::*kan*) versus the wild type directly on the array, RB35 (Δ*smc*::*kan*) versus RB25 (*ftsY*::pDL53), and RB27 (*smc*::pRB7) versus RB25 (*ftsY*::pDL53)].

Changes in gene expression that occurred in all three strains (RB25, RB27, and RB35) relative to the wild type were likely caused by decreased expression

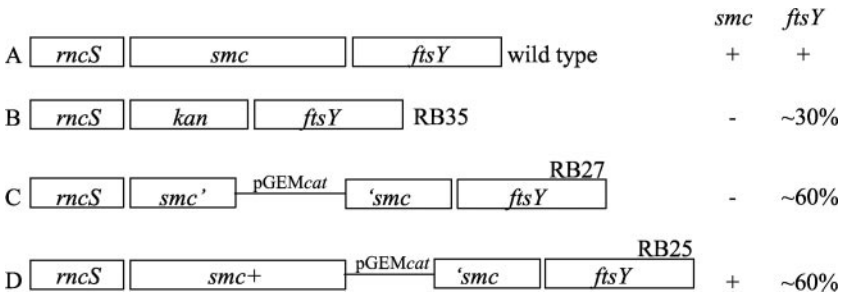

FIG. 1. Genomic configurations of *smc* and *ftsY* mutations. (A) Wild-type operon structure of *rncS-smc-ftsY*. (B) Strain RB35 Δ*smc*::*kan* (deletion in *smc* with insertion of the kanamycin resistance gene *kan*) (5). This causes an *smc* null phenotype and reduced expression of *ftsY*. Levels of *ftsY* mRNA ranged from approximately 30% to 55% of that of the wild type. (C) Strain RB27 (single crossover of pRB27 causing disruption of *smc* and insertion of pGEM*cat*). This causes an *smc* null phenotype and reduced expression of *ftsY* (~55 to 60% of that of the wild type). (D) Strain RB25 (a single crossover of pDL53, containing pGEM*cat*, into *ftsY*, causing insertion of pGEM*cat* between *smc* and *ftsY*) (5). This causes reduced expression of *ftsY* (~55 to 60% of that of the wild type), while leaving *smc* intact. The 3′ fragments of *smc* preceding *ftsY* in RB27 and RB25 are identical. The *smc* phenotype of each strain is indicated to the right: +, wild type; −, null. The approximate amount of *ftsY* mRNA relative to the wild type is also indicated.

of *ftsY*, because that is the only mutation common to all three strains. There were 60 genes with altered mRNA levels in all three strains with decreased expression of *ftsY* (see Table S1 in the supplemental material), indicative of the significant effects of FtsY on gene expression. This is probably an underestimate of the effects of *ftsY*, since some effects might be masked (or compensated for) due to the loss of *smc* in strains RB27 and RB35. Preliminary analysis of alterations due to decreased expression of *ftsY*, without altering *smc*, indicates that perhaps 300 genes are affected. This analysis is beyond the scope of this study, and we have not pursued it further.

Microscopy. Analyses of green fluorescent protein (GFP) fusions in live cells were done by spotting cells onto slides coated with a thin agarose pad (1× TBase, 1% $MgSO_4$), as previously described (22). Cells were imaged with a Nikon E800 epifluorescence microscope.

Microarray data accession number. Microarray data have been submitted to the GEO database under series record GSE5210.

RESULTS

Effects of *smc* null mutations on gene expression. We used whole-genome microarrays to determine the effects of null mutations in *smc* on the levels of mRNA for virtually all open reading frames in the *B. subtilis* genome (3). Analysis of mRNA levels from several strains and several replicates indicated that *smc* null mutations cause a partial induction of the SOS response.

Initially, we directly compared mRNA profiles from the wild type (AG174) and an *smc* null mutant (RB35). Cells were grown in defined minimal medium at 30°C to mid-exponential phase. Under these growth conditions, the *smc* mutant produced ~10% anucleate cells and grew ~50% slower than did wild-type cells (5). Cells were harvested, and RNA was isolated and prepared for hybridization to genomic microarrays (see Materials and Methods).

Analysis of the microarray data from four independently grown pairs of cultures showed that approximately 275 genes were differentially expressed between the two strains. However, the *smc* null allele is a large deletion in *smc* with insertion of a kanamycin resistance cassette. In these experiments, expression of *ftsY*, the gene immediately downstream of *smc*, was reduced to approximately 30% of that of the wild type (~3.4-fold down), indicating that the Δ*smc*::*kan* allele is partly polar on *ftsY*. These results make it difficult to assign the observed changes specifically to the disruption of *smc*. Therefore, we performed additional experiments to measure the effects of reducing the amount of expression of *ftsY* and to account for these effects in our analysis of the effects of disrupting *smc*.

ftsY (also known as *srb*) encodes an essential component of the signal recognition particle that is involved in secretion of many proteins during growth and sporulation (19). We were concerned that even small changes in expression of *ftsY* might affect the mRNA levels of many genes. Due to potential alterations in mRNA structure and stability, and translational coupling and efficiency, even "nonpolar" mutations can have effects on the expression of downstream genes. To take into account potential effects on expression of *ftsY* caused by mutations in *smc*, we measured the effects caused by two alleles that should have identical effects on *ftsY*. One allele, *smc*::pRB7 (RB27), is an *smc* null mutation that affects *ftsY* expression. The other allele, smc^+ *ftsY*::pDL53 (RB25) is smc^+ but also causes decreased transcription of *ftsY*, like *smc*::pRB7 (Fig. 1). Both of these alleles cause *ftsY* mRNA to be ~55 to 60% of that in wild-type cells, an effect less severe than that caused by the Δ*smc*::*kan* mutation (Fig. 1).

There were 36 genes whose expression appeared to be specifically and significantly altered due to loss of *smc* (Table 2). Expression of all of these genes was increased in the *smc* mutant. Most noticeable was the increased expression of genes of the defective prophage PBSX and the integrative and conjugative element ICE*Bs1*. Table 2 also includes genes from these elements that appeared to be affected in our experiments but not in a statistically significant way. Both of these elements are significantly induced by the SOS response (2, 12, 13, 28).

The *smc* null mutations also caused increased expression of *dinB* (Table 2). *dinB* is DNA damage inducible, highly expressed during the SOS response, and directly repressed by LexA (1, 7, 11, 12), the major repressor of the RecA-dependent SOS response. In addition to *dinB*, two other genes, *tagC* (also known as *dinC*) and *lexA*, that are directly repressed by LexA were identified as increased in the *smc* mutants in some of our experiments, but these effects were not consistent enough to meet the statistical criteria. Expression of *ybfG* was also increased in the *smc* mutants. *ybfG* is not known to have a LexA binding site (1). However, it is induced during the SOS response, and its induction is *recA* dependent and appears to be dependent on the induction of ICE*Bs1* or the phage PBSX or SPβ (12).

We also observed induction of genes of the prophage SPβ in some of the experiments with the *smc* null mutants. However, these results were somewhat variable between experiments, did not meet the statistical criteria, and are not included in the analysis. SPβ is known to be induced during the SOS response (12, 29).

Taken together, the results indicate that the SOS response is induced in the *smc* null mutant. However, in *B. subtilis*, a fully induced SOS response, for example, following treatment of cells with a DNA-damaging agent, involves changes in expression of hundreds of genes, some increasing and others decreasing (12, 13). Furthermore, expression of many of the genes that are normally induced during SOS is typically much greater than that observed in the *smc* null mutants. The relatively modest levels of increased gene expression and the limited number of genes affected in the *smc* mutant indicate that there is either poor induction in all cells or significant induction in a small subpopulation of cells (see below). That we do not see decreased expression of any genes is consistent with these possibilities.

We also noticed significant and reproducible effects of *smc* on expression of *clpE*, *yrhH*, and *yxlC* (Table 2). The *clpE* gene product contributes to the regulation of one of the repressors (CtsR) of the heat shock response, is probably involved in global protein disaggregation, and is induced by heat shock (8, 30). *yrhH* encodes a putative methyltransferase that was found to be induced in response to an antimicrobial cationic peptide (33). *yxlC* encodes a protein of unknown function and is immediately downstream from and cotranscribed with *sigY*. *sigY* encodes an ECF-type sigma factor, and polar mutations in *yxlC* (due to effects on downstream genes) cause increased activity of SigY (6). Neither *sigY* nor the downstream genes apparently cotranscribed with *yxlC* were identified as having altered expression in the *smc* mutant. We have not explored this appar-

TABLE 2. Genes whose expression is affected in *smc* null mutants

Gene[a]	Fold change[b]	*topA* effect (fold change)[c]	Function or mobile element[d]
clpE	12.2	1.6	ATP-dependent Clp protease-like (class III stress gene)
dinB	2.8	2.8	Nuclease inhibitor
xkdB	2.5	1.9	PBSX
xkdC	3.4	4.0	PBSX
xkdD	3.6	5.7	PBSX
xtrA	2.0	3.2	PBSX
xpf	3.0	5.6	PBSX
xtmA	9.5	8.2	PBSX
xtmB	8.5	7.5	PBSX
xkdE	9.3	11.1	PBSX
xkdF	14.6	11.8	PBSX
xkdG	13.1	13.6	PBSX
xkdH	6.4	5.1	PBSX
xkdI	5.4	4.4	PBSX
xkdJ	11.7	7.4	PBSX
xkdK	9.8	9.8	PBSX
xkdM	12.4	8.2	PBSX
xkdN	13.3	13.1	PBSX
xkdO	3.0	2.9	PBSX
xkdP	6.6	7.1	PBSX
xkdQ	8.4	5.2	PBSX
xkdR	4.5	8.3	PBSX
xkdS	5.5	6.1	PBSX
xkdT	7.4	7.7	PBSX
xkdU	7.0	8.4	PBSX
xkdV	10.0	7.1	PBSX
xkdW	6.3	7.1	PBSX
xkdX	3.8	8.0	PBSX
xepA	12.1	8.5	PBSX
xhlA	16.6	5.7	PBSX
xhlB	7.9	5.0	PBSX
xlyA	13.6	6.6	PBSX
xlyB	6.8	7.4	PBSX
ybfG	5.3	6.2	Probable membrane protein; similar to unknown proteins
ydcO	3.0	1.3	ICE*Bs1* (2)
ydcP	3.9	6.5	ICE*Bs1*
ydcQ	6.3	5.6	ICE*Bs1*
ydcR	5.3	5.4	ICE*Bs1*
ydcS	3.1	9.2	ICE*Bs1*
ydcT	1.9	10.6	ICE*Bs1*
yddA	1.9	10.6	ICE*Bs1*
yddB	3.8	3	ICE*Bs1*
yddC	2.1	5.7	ICE*Bs1*
yddD	2.9	6.5	ICE*Bs1*
yddE	2.0	7.0	ICE*Bs1*
yddF	1.8	2.3	ICE*Bs1*
yddG	2.1	1.9	ICE*Bs1*
yddH	1.8	3.5	ICE*Bs1*
yddI	2.0	ND	ICE*Bs1*
yrhH	6.7	ND	Unknown; similar to methyltransferase
yxlC	6.0	ND	Unknown

[a] Gene names are from Subtilist (http://genolist.pasteur.fr/SubtiList/). Genes are listed in the order they appear on the chromosome in predicted operons. Genes likely to be coregulated include genes of the PBSX prophage (39, 40) and genes of the integrative and conjugative element ICE*Bs1* (2). Genes shown in boldface type were significantly and reproducibly altered in expression in the *smc* mutants. Average mRNA levels were 2.5 standard deviations from the mean of the population in the *smc* mutants in the iterative outlier analysis. Other genes of PBSX and ICE*Bs1* are included in plain text for comparison. Their expression was typically increased in the mutants in some experiments but was not reproducible enough to meet the statistical criteria. They are included because they are generally coregulated with the other genes of the element. *smc* and *ftsY* are not shown, as they are the mutant alleles. Also not shown are several genes in the *skin* element, a defective phage integrated into *sigK*. These genes have over 90% identity to genes of PBSX (20); because only the genes in the *skin* element that were highly similar to PBSX were increased in expression, it is likely that these genes cross-hybridized with PBSX transcripts, as previously described (12).

[b] Largest average fold change in mRNA levels in an *smc* null mutant compared to *smc*$^+$ cells.

[c] Average fold change of gene expression upon decreased expression of *topA* (Topo I) from P_{spac}-*topA* (strain JCL245 grown without and with IPTG in defined minimal medium at 30°C; the full set of genes affected is presented in Table S2 in the supplemental material). ND, no data for the indicated gene.

[d] Indicates function described in Subtilist or location in the mobile element PBSX or ICE*Bs1* (2).

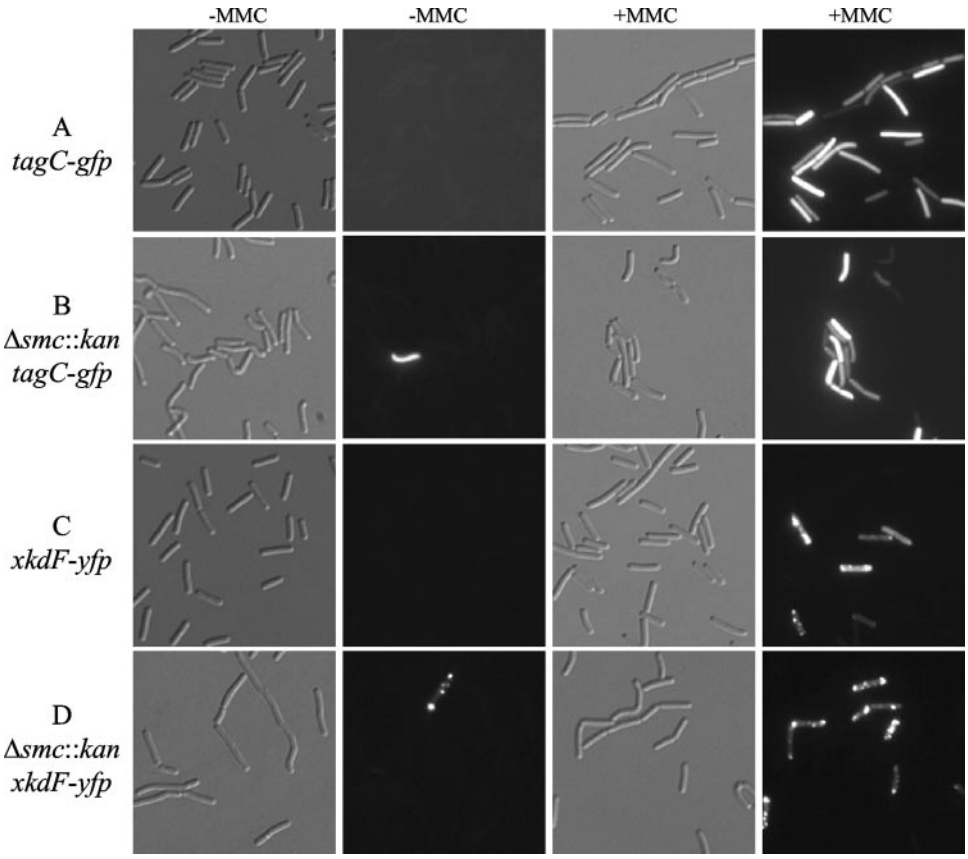

FIG. 2. Fluorescence microscopy of cells containing *tagC-gfp* (SOS response) or *xkdF-yfp* (PBSX). Cells were grown in defined minimal medium at 30°C and sampled for microscopy in mid-exponential phase. Samples were taken 90 min after the addition of MMC (1 μg/ml). Columns 1 and 3 are differential interference contrast images of bacterial cells. Columns 2 and 4 are fluorescence images (of the same field) of either GFP or YFP. Columns 1 and 2 show untreated cells (−MMC); columns 3 and 4 show cells treated with 1 μg/ml MMC. Rows: A, strain RB98 (*tagC-gfp*); B, strain RB169 (Δ*smc*::*kan tagC-gfp*); C, strain RB178 (*xkdF-yfp*); D, strain RB164 (Δ*smc*::*kan xkdF-yfp*).

ent discrepancy, nor do we understand how *smc* affects the expression of *yxlC*, *yrhH*, and *clpE*.

We did not detect effects of *smc* on expression of *sacB* or any of the other genes in the DegS-DegU regulon. DegS is a histidine protein kinase that modulates the activity of the transcription factor DegU, a response regulator. Smc and ScpA were previously found to regulate the expression of *sacB* and perhaps the entire DegS-DegU regulon, and interaction between ScpA and DegS was detected in a yeast two-hybrid assay (9). Our experiments were done under conditions in which DegS-DegU would not normally be active, so we did not expect to observe this regulation.

PBSX is induced in a small subpopulation of *smc* mutant cells. Induction of PBSX does not produce active phage particles but does lead to lysis of the cells in which it is induced (28). If the *smc* mutation caused induction of PBSX in all cells, then *smc* null mutants should not be viable. Because *smc* mutants are viable (although sick), we expected that only a subpopulation of cells was inducing PBSX and that perhaps only a subpopulation was inducing the SOS response.

To determine the fraction of cells inducing PBSX, we visualized induction of PBSX at the single-cell level. We fused *xkdF*, a gene in PBSX, to *yfp*, creating an *xkdF-yfp* fusion (see Materials and Methods). To test whether XkdF-yellow fluorescent protein (YFP) could be used as a marker for PBSX induction, a wild-type strain containing *xkdF-yfp* was treated with MMC. Approximately 13% of these cells had bright fluorescent foci, ranging in number from one to several foci per cell (Fig. 2; Table 3). The function of *xkdF* in PBSX biology is not known, and we do not know the function of the foci. In the absence of MMC, we did not observe any cells (0 of 1,698 cells visualized) with XkdF-YFP foci. These results indicate that XkdF-YFP can be used as a marker for induction of PBSX.

We determined the fraction of *smc* mutant cells expressing *xkdF-yfp*. Cells were grown in defined minimal medium, and samples were taken during exponential growth and analyzed by fluorescence microscopy. We found that ~1% of *smc* null mutant cells had visible foci of XkdF-YFP, indicating that ~1% of cells had fully induced PBSX (Fig. 2; Table 3). When the *smc xkdF-yfp* strain was treated with MMC, almost 60% of the cells had XkdF-YFP foci, whereas when the *smc*$^+$ *xkdF-yfp* strain was treated with MMC, ~13% of the cells had XkdF-YFP foci (Table 3). This increase in the induction of PBSX in the *smc* mutant is consistent with the finding that *smc* null mutants are more sensitive to MMC (9).

To be sure that the induction of PBSX and expression of *xkdF-yfp* was due to *smc* and not to decreased expression of *ftsY*,

TABLE 3. Analysis of *tagC*-GFP (SOS) and *xkdF*-YFP (PBSX) expression in single cells[a]

Genotype (strain)[b]	% of cells expressing fusion[c]	
	Without MMC	With MMC
Wild type, *tagC-gfp* (RB98)	<0.02 (0/5,000)	>99
Δ*smc tagC-gfp* (RB169)	1.6 (23/1,425)	>99
Wild type, *xkdF-yfp* (RB178)	<0.06 (0/1,698)	13.4 (133/992)
Δ*smc xkdF-yfp* (RB164)	0.91 (43/4,743)	57.5 (1,072/1,863)
Δ*scpA xkdF-yfp* (RB179)	0.94 (24/2,549)	ND
P_{spac}-*topA xkdF-yfp* (RB243)[d]	1.2 (30/2,471)	ND
ftsY::pDL53 *xkdF-yfp* (RB244)	<0.05 (1/2,148)	ND

[a] All cells were grown to mid-exponential phase in defined minimal medium at 30°C. Cells were prepared for microscopy at an OD_{600} of 0.5 to 0.8. For cultures treated with MMC, cells were grown to an OD_{600} of 0.5 to 0.7, at which point 1 μg/ml of MMC was added. After 90 min, cells were prepared for microscopy.

[b] Relevant genotype and fusion are indicated.

[c] Percentage of cells expressing the indicated GFP or YFP fusion. Values in parentheses are the number of fluorescent cells observed over the total number of cells observed. ND, not determined.

[d] Grown in the absence of IPTG, causing decreased expression of *topA* and decreased amounts of Topo I.

we analyzed *xkdF-yfp* expression in the *smc*$^+$ strain that had decreased expression of *ftsY*, strain RB25 (*ftsY*::pDL53), which was used for the gene expression analysis. In this mutant, <0.05% of the cells had visible foci of XkdF-YFP (Table 3). We also visualized expression of *xkdF-yfp* in an *scpA* null mutant. Phenotypes of an *scpA* mutant are similar to those of an *smc* mutant (24, 35). As expected, we found that ~1% of the *scpA* mutant cells had visible foci of XkdF-YFP (Table 3). Together, these results indicate that induction of PBSX occurs in ~1% of *smc* (or *scpA*) mutant cells and that this induction is due to loss of Smc function and not to decreased expression of *ftsY*.

The SOS response is induced in a small subpopulation of *smc* mutant cells. Based on the gene expression results from the DNA microarray experiments and the single-cell analysis of PBSX gene expression, we suspected that the SOS response was induced in a subpopulation of *smc* mutant cells. To test this, we analyzed the expression of an SOS-inducible gene, *tagC* (*dinC*), in individual cells. *tagC* was fused to *gfp* and transformed into wild-type or *smc* mutant strains. To verify that *tagC-gfp* could be used as a marker for SOS, a wild-type strain containing the *tagC-gfp* fusion was grown in defined minimal medium at 30°C to mid-exponential phase. The culture was split, and MMC (1 μg/ml) was added to one of the flasks. After 90 min, cells were analyzed by fluorescence microscopy for expression of TagC-GFP. Nearly 100% of the cells treated with MMC had significant fluorescence from the TagC-GFP fusion. The level of expression was variable between cells, indicating different levels of induction. We observed no cells (of approximately 5,000) with detectable fluorescence over background in the untreated culture. These results indicate that TagC-GFP can be used to monitor induction of the SOS response.

We found that ~1% of the *smc* null mutant cells had visible expression of *tagC-gfp*, indicating that the SOS response was induced in these cells. *smc* mutant cells were grown to mid-exponential phase and prepared for fluorescence microscopy. Cells that were clearly fluorescent above the background of the population were evident (Fig. 2). The frequency of *smc* mutant cells with significant expression of *tagC-gfp* (~1%) was similar to the frequency of mutant cells with induction of PBSX (Table 3).

Phage induction and the *smc* null phenotype. We were interested in determining whether induction of phage or ICE*Bs1* contributed to the defects in growth rate, chromosome partitioning and compaction, and induction of the SOS response in the *smc* null mutant. To test this, we analyzed the phenotypes caused by an *smc* null mutation in strains cured of SPβ and ICE*Bs1* and in the strain unable to induce the defective phage PBSX, strain YB886 (2, 40). The mutation *xin-1* renders the defective phage uninducible (39, 40). The absence of SPβ and ICE*Bs1* and the inability to induce PBSX had no detectable effect on the phenotypes caused by null mutations in *smc*, including doubling time, anucleate cell production, or the appearance of decompacted chromosomes (data not shown).

We also monitored mRNA levels in *smc* and *scpA* null mutants that are also defective in phage induction, including Δ*smc*::*kan xin-1* SPβ^0 *xkdF-yfp* (RB177), Δ*smc*::*kan xin-1* SPβ^0 (RB151), and Δ*scpA xin-1* SPβ^0 *xkdF-yfp* (RB175) strains, none of which can express PBSX due to the presence of the *xin-1* mutation. In single microarray experiments with each strain, the *smc* or *scpA* null mutants still had increased expression of SOS genes. Expression of *lexA*, *dinB*, and *tagC* was increased two- to eightfold in PBSX-uninducible *smc* (and *scpA*) mutant strains (data not shown). As expected, we did not detect any induction of PBSX in these strains. These results indicate that SOS induction in the *smc* mutant occurs in the absence of PBSX induction.

Increased negative supercoiling causes induction of the SOS response. Previous work demonstrated that plasmid DNA isolated from *smc* null mutants is more negatively supercoiled in the cell, most likely due to the loss of Smc constraining positive supercoils in DNA (23). Topo I (encoded by *topA*) relaxes negative supercoils in DNA, and the loss of Topo I function causes DNA to be more negatively supercoiled (10). To evaluate the effects of supercoiling on global gene expression, we analyzed changes in mRNA isolated from cells depleted of Topo I and compared these changes to those caused by the *smc* null mutation.

Cells depleted of Topo I, due to decreased expression of *topA*, had a mild induction of the SOS response and induction of the PBSX prophage, similar to what was found with the *smc* strain. Expression of approximately 300 genes was altered in cells depleted for Topo I (see Table S2 in the supplemental material). Part of the reason for so many more additional genes being found in Topo I-depleted cells than in *smc* mutants was that the phage SPβ was more strongly induced in Topo I-depleted cells. Approximately 100 genes of SPβ that were not detected in *smc* mutant cells were found to be changed (although in some individual experiments we did see some of the genes being induced in the *smc* mutant, this was not a consistent observation and genes of SPβ did not show up as significantly and reproducibly changed in our final analysis). The changes observed in the genes of PBSX and the SOS response were quite similar in both Topo I-depleted and *smc* mutant cells.

Single-cell induction of PBSX was analyzed in cells depleted for Topo I, with XkdF-YFP used as a marker. Induction of PBSX occurred in 1.2% of the cells, similar to what was found in *smc* mutant cells (Table 3). These data indicate that in-

creased negative supercoiling in *B. subtilis* cells can also lead to the SOS response and induction of PBSX.

DISCUSSION

Altered gene expression in *smc mutants*. DNA microarray analysis of gene expression in *smc* null mutants indicated that there was partial induction of the SOS response, including increased expression of a few genes repressed by LexA and increased induction of the defective prophage PBSX. In *B. subtilis*, a robust SOS response to DNA damage affects expression of about 500 genes, most of which are induced and depend on *recA* (12). Analysis of gene expression in single cells indicated that the increased expression of PBSX and SOS genes was due to apparently full expression in a subpopulation (~1%) of the *smc* mutant cells. It is likely that induction of SOS in the *smc* mutants leads to induction of PBSX, as the SOS response is known to induce PBSX (12, 39, 40).

Analysis of mutants that can no longer induce PBSX showed that the likely order of events is induction of the SOS response that then leads to phage induction. Induction of the SOS response in a small population of *smc* null mutant cells is similar to what has been observed in several mutants that affect DNA metabolism in *E. coli* (27). McCool et al. suggest that the induction of the SOS response in a subpopulation of cells is likely due to the fact that not all of the cells had a significant DNA-damaging event and/or needed the missing protein (27). We envision a similar scenario for *smc* mutants. That is, we suspect that in ~1% of the population, enough DNA damage occurs to cause induction of the SOS response.

Phage induction had no effect on the phenotypes observed in *smc* null mutants. *smc* mutants that lack SPβ and the ability to induce PBSX still had slow growth, temperature sensitivity, abnormal nucleoid morphology, and a similar percentage of anucleate cells. Attempts to construct *smc recA* double mutants to test the effects of the *recA*-dependent SOS response on the phenotypes caused by *smc* null mutations were unsuccessful.

Effects of Topo I on gene expression. We also analyzed changes in gene expression that occur when Topo I is depleted from cells. The results indicate that induction of the SOS response in *smc* mutants could be due to increased negative supercoiling. Topo I is a type I topoisomerase that relaxes negative supercoils in bacteria; removal of this activity leads to hyper-negatively supercoiled DNA in the cell. Depletion of Topo I caused activation of the SOS response and PBSX induction in a subpopulation of the cells; ~1% of cells had induced PBSX, similar to what occurs in the *smc* mutants. This indicates that hyper-negatively supercoiled DNA can, in some instances, lead to activation of the SOS response.

***smc and scp* mutants and sensitivity to MMC.** Previously it was reported that mutations in *smc* and *scpA* cause cells to be more sensitive to the DNA-damaging agent MMC (9). We confirmed that Δ*smc* mutants are more sensitive to MMC and suspect that this susceptibility is due to altered compaction of DNA in *smc* mutants, resulting in DNA damage. Increased sensitivity to MMC correlated with increased production of anucleate cells in various *scpA* mutants (9), consistent with a role for altered chromosome compaction in sensitivity to MMC. Alternatively, it was proposed that the increased sensitivity of *scpA* mutants to MMC is due to altered interaction with AddB (9). AddB is involved in recombination and DNA repair. Increased expression of AddAB suppressed the increased sensitivity of *scpA* missense mutants (but not of *scpA* or *smc* null mutants) to MMC, indicating that the increased sensitivity might be due to loss of recruitment of AddAB by the Smc-Scp complex to sites of DNA damage (9). More studies are needed to understand the role of the Smc-Scp complex in DNA damage and repair.

Altered supercoiling and the SOS response. The mechanism by which the SOS response is induced in *smc* mutants is not known. The fact that cells depleted for Topo I have a similar increase in expression of the SOS response indicates that hyper-negatively supercoiled DNA could be responsible for the phenotype. Topo I-depleted cells and *smc* null mutants do not share other phenotypes, such as production of anucleate cells or guillotined chromosomes. Therefore, it seems unlikely that the SOS response is being induced by improper segregation of the chromosome and that the defect is more likely to be due to altered compaction of the DNA due to altered supercoiling.

The SOS response is activated by the presence of single-stranded DNA, which can be generated in many different ways. In a growing culture, there are always cells that are experiencing replication fork arrest. The loss of Smc function could prolong this arrest, perhaps by delaying replication restart, causing generation of single-stranded DNA and induction of SOS in that subpopulation of cells. In addition, the chromosomes of *smc* null mutants might be more susceptible to double-stranded DNA breaks, which are then rapidly metabolized into single-stranded DNA. The defect in chromosome compaction caused by loss of Smc function could cause local denaturing of DNA, causing extensive single-stranded regions. When DNA is underwound, the tension caused can be alleviated by negative supercoiling or by local unwinding of the DNA. The latter process results in generating single-stranded regions of DNA. Interestingly, condensin from yeast, as well as *B. subtilis* Smc, has been shown to have the ability to renature denatured DNA (15, 36). Compaction by bacterial condensin (SMC and associated proteins) could prevent localized unwinding of the chromosome. These possible mechanisms are not exclusive, and we suspect that they all contribute to SOS activation in a subpopulation of *smc* mutant cells.

ACKNOWLEDGMENTS

We thank Janet Lindow for helping with the construction of the *xkdF-yfp* fusion and members of the Grossman lab for useful discussions and comments on the manuscript.

R.A.B. was supported in part by a postdoctoral fellowship from the NIH. This work was also supported in part by NIH grant GM41934 to A.D.G.

REFERENCES

1. **Au, N., E. Kuester-Schoeck, V. Mandava, L. E. Bothwell, S. P. Canny, K. Chachu, S. A. Colavito, S. N. Fuller, E. S. Groban, L. A. Hensley, T. C. O'Brien, A. Shah, J. T. Tierney, L. L. Tomm, T. M. O'Gara, A. I. Goranov, A. D. Grossman, and C. M. Lovett.** 2005. Genetic composition of the *Bacillus subtilis* SOS system. J. Bacteriol. **187:**7655–7666.
2. **Auchtung, J. M., C. A. Lee, R. E. Monson, A. P. Lehman, and A. D. Grossman.** 2005. Regulation of a Bacillus subtilis mobile genetic element by intercellular signaling and the global DNA damage response. Proc. Natl. Acad. Sci. USA **102:**12554–12559.
3. **Britton, R. A., P. Eichenberger, J. E. Gonzalez-Pastor, P. Fawcett, R. Monson, R. Losick, and A. D. Grossman.** 2002. Genome-wide analysis of the stationary-phase sigma factor (σ^H) regulon of *Bacillus subtilis*. J. Bacteriol. **184:**4881–4890.
4. **Britton, R. A., and A. D. Grossman.** 1999. Synthetic lethal phenotypes caused

by mutations affecting chromosome partitioning in *Bacillus subtilis*. J. Bacteriol. **181:**5860–5864.
5. **Britton, R. A., D. C. Lin, and A. D. Grossman.** 1998. Characterization of a prokaryotic SMC protein involved in chromosome partitioning. Genes Dev. **12:**1254–1259.
6. **Cao, M., L. Salzberg, C. S. Tsai, T. Mascher, C. Bonilla, T. Wang, R. W. Ye, L. Marquez-Magana, and J. D. Helmann.** 2003. Regulation of the *Bacillus subtilis* extracytoplasmic function protein σ^Y and its target promoters. J. Bacteriol. **185:**4883–4890.
7. **Cheo, D. L., K. W. Bayles, and R. E. Yasbin.** 1991. Cloning and characterization of DNA damage-inducible promoter regions from *Bacillus subtilis*. J. Bacteriol. **173:**1696–1703.
8. **Derre, I., G. Rapoport, K. Devine, M. Rose, and T. Msadek.** 1999. ClpE, a novel type of HSP100 ATPase, is part of the CtsR heat shock regulon of Bacillus subtilis. Mol. Microbiol. **32:**581–593.
9. **Dervyn, E., M. F. Noirot-Gros, P. Mervelet, S. McGovern, S. D. Ehrlich, P. Polard, and P. Noirot.** 2004. The bacterial condensin/cohesin-like protein complex acts in DNA repair and regulation of gene expression. Mol. Microbiol. **51:**1629–1640.
10. **Giaever, G. N., L. Snyder, and J. C. Wang.** 1988. DNA supercoiling in vivo. Biophys. Chem. **29:**7–15.
11. **Gillespie, K., and R. E. Yasbin.** 1987. Chromosomal locations of three *Bacillus subtilis din* genes. J. Bacteriol. **169:**3372–3374.
12. **Goranov, A., E. Kuester-Schoeck, J. Wang, and A. Grossman.** 2006. Characterization of the global transcriptional responses to different types of DNA damage and disruption of replication in *Bacillus subtilis*. J. Bacteriol. **188:** 5595–5605.
13. **Goranov, A. I., L. Katz, A. M. Breier, C. B. Burge, and A. D. Grossman.** 2005. A transcriptional response to replication status mediated by the conserved bacterial replication protein DnaA. Proc. Natl. Acad. Sci. USA **102:**12932–12937.
14. **Haering, C. H., and K. Nasmyth.** 2003. Building and breaking bridges between sister chromatids. Bioessays **25:**1178–1191.
15. **Hirano, M., and T. Hirano.** 1998. ATP-dependent aggregation of single-stranded DNA by a bacterial SMC homodimer. EMBO J. **17:**7139–7148.
16. **Hirano, T.** 2005. SMC proteins and chromosome mechanics: from bacteria to humans. Philos. Trans. R. Soc. Lond. B **360:**507–514.
17. **Hirano, T.** 2002. The ABCs of SMC proteins: two-armed ATPases for chromosome condensation, cohesion, and repair. Genes Dev. **16:**399–414.
18. **Jessberger, R.** 2002. The many functions of SMC proteins in chromosome dynamics. Nat. Rev. Mol. Cell Biol. **3:**767–778.
19. **Kakeshita, H., A. Oguro, R. Amikura, K. Nakamura, and K. Yamane.** 2000. Expression of the *ftsY* gene, encoding a homologue of the alpha subunit of mammalian signal recognition particle receptor, is controlled by different promoters in vegetative and sporulating cells of Bacillus subtilis. Microbiology **146:**2595–2603.
20. **Krogh, S., M. O'Reilly, N. Nolan, and K. M. Devine.** 1996. The phage-like element PBSX and part of the skin element, which are resident at different locations on the Bacillus subtilis chromosome, are highly homologous. Microbiology **142:**2031–2040.
21. **Lee, P. S., and A. D. Grossman.** 2006. The chromosome partitioning proteins Soj (ParA) and Spo0J (ParB) contribute to accurate chromosome partitioning, separation of replicated sister origins, and regulation of replication initiation in Bacillus subtilis. Mol. Microbiol. **60:**853–869.
22. **Lemon, K. P., and A. D. Grossman.** 1998. Localization of bacterial DNA polymerase: evidence for a factory model of replication. Science **282:**1516–1519.
23. **Lindow, J. C., R. A. Britton, and A. D. Grossman.** 2002. Structural maintenance of chromosomes protein of *Bacillus subtilis* affects supercoiling in vivo. J. Bacteriol. **184:**5317–5322.
24. **Lindow, J. C., M. Kuwano, S. Moriya, and A. D. Grossman.** 2002. Subcellular localization of the Bacillus subtilis structural maintenance of chromosomes (SMC) protein. Mol. Microbiol. **46:**997–1009.
25. **Loos, A., C. Glanemann, L. B. Willis, X. M. O'Brien, P. A. Lessard, R. Gerstmeir, S. Guillouet, and A. J. Sinskey.** 2001. Development and validation of *Corynebacterium* DNA microarrays. Appl. Environ. Microbiol. **67:** 2310–2318.
26. **Mascarenhas, J., J. Soppa, A. V. Strunnikov, and P. L. Graumann.** 2002. Cell cycle-dependent localization of two novel prokaryotic chromosome segregation and condensation proteins in Bacillus subtilis that interact with SMC protein. EMBO J. **21:**3108–3118.
27. **McCool, J. D., E. Long, J. F. Petrosino, H. A. Sandler, S. M. Rosenberg, and S. J. Sandler.** 2004. Measurement of SOS expression in individual Escherichia coli K-12 cells using fluorescence microscopy. Mol. Microbiol. **53:** 1343–1357.
28. **McDonnell, G. E., H. Wood, K. M. Devine, and D. J. McConnell.** 1994. Genetic control of bacterial suicide: regulation of the induction of PBSX in *Bacillus subtilis*. J. Bacteriol. **176:**5820–5830.
29. **McVeigh, R. R., and R. E. Yasbin.** 1996. Phenotypic differentiation of "smart" versus "naive" bacteriophages of *Bacillus subtilis*. J. Bacteriol. **178:** 3399–3401.
30. **Miethke, M., M. Hecker, and U. Gerth.** 2006. Involvement of *Bacillus subtilis* ClpE in CtsR degradation and protein quality control. J. Bacteriol. **188:** 4610–4619.
31. **Moriya, S., E. Tsujikawa, A. K. Hassan, K. Asai, T. Kodama, and N. Ogasawara.** 1998. A *Bacillus subtilis* gene-encoding protein homologous to eukaryotic SMC motor protein is necessary for chromosome partition. Mol. Microbiol. **29:**179–187.
32. **Pedersen, L. B., and P. Setlow.** 2000. Penicillin-binding protein-related factor A is required for proper chromosome segregation in *Bacillus subtilis*. J. Bacteriol. **182:**1650–1658.
33. **Pietiainen, M., M. Gardemeister, M. Mecklin, S. Leskela, M. Sarvas, and V. P. Kontinen.** 2005. Cationic antimicrobial peptides elicit a complex stress response in Bacillus subtilis that involves ECF-type sigma factors and two-component signal transduction systems. Microbiology **151:**1577–1592.
34. **Soppa, J.** 2001. Prokaryotic structural maintenance of chromosomes (SMC) proteins: distribution, phylogeny, and comparison with MukBs and additional prokaryotic and eukaryotic coiled-coil proteins. Gene **278:**253–264.
35. **Soppa, J., K. Kobayashi, M. F. Noirot-Gros, D. Oesterhelt, S. D. Ehrlich, E. Dervyn, N. Ogasawara, and S. Moriya.** 2002. Discovery of two novel families of proteins that are proposed to interact with prokaryotic SMC proteins, and characterization of the Bacillus subtilis family members ScpA and ScpB. Mol. Microbiol. **45:**59–71.
36. **Sutani, T., and M. Yanagida.** 1997. DNA renaturation activity of the SMC complex implicated in chromosome condensation. Nature **388:**798–801.
37. **Vasantha, N., and E. Freese.** 1980. Enzyme changes during *Bacillus subtilis* sporulation caused by deprivation of guanine nucleotides. J. Bacteriol. **144:** 1119–1125.
38. **Volkov, A., J. Mascarenhas, C. Andrei-Selmer, H. D. Ulrich, and P. L. Graumann.** 2003. A prokaryotic condensin/cohesin-like complex can actively compact chromosomes from a single position on the nucleoid and binds to DNA as a ring-like structure. Mol. Cell. Biol. **23:**5638–5650.
39. **Yasbin, R. E.** 1977. DNA repair in Bacillus subtilis. II. Activation of the inducible system in competent bacteria. Mol. Gen. Genet. **153:**219–225.
40. **Yasbin, R. E., P. I. Fields, and B. J. Andersen.** 1980. Properties of Bacillus subtilis 168 derivatives freed of their natural prophages. Gene **12:**155–159.